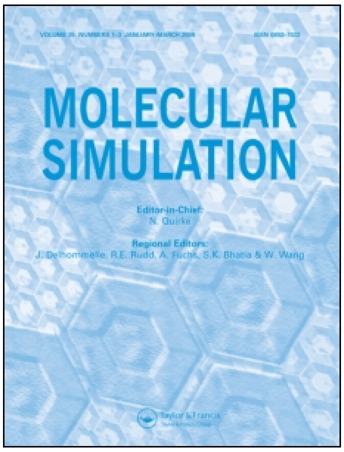

Molecular Simulation

Publication details, including instructions for authors and subscription information:
http://www.informaworld.com/smpp/title~content=t713644482

Cation transport in nanopores

J. Marañón Di Leo[a]; J. Marañón[b]
[a] Departamento de Aeronáutica, Facultad de Ingeniería, Universidad Nacional de La Plata, La Plata, Argentina [b] IFLP, Departamento de Física, Facultad de Ciencias Exactas, Universidad Nacional de La Plata, La Plata, Argentina

To cite this Article Marañón Di Leo, J. and Marañón, J.(2009) 'Cation transport in nanopores', Molecular Simulation, 35: 4, 280 — 286

To link to this Article: DOI: 10.1080/08927020802488073

URL: http://dx.doi.org/10.1080/08927020802488073

Molecular Simulation
Vol. 35, No. 4, April 2009, 280–286

Taylor & Francis
Taylor & Francis Group

Cation transport in nanopores

J. Marañón Di Leo[a] and J. Marañón[b]*

[a]*Departamento de Aeronáutica, Facultad de Ingeniería, Universidad Nacional de La Plata, La Plata, Argentina;* [b]*IFLP, Departamento de Física, Facultad de Ciencias Exactas, Universidad Nacional de La Plata, La Plata, Argentina*

(*Received 19 June 2008; final version received 17 September 2008*)

Using periodic boundary conditions and external electric potential field, we have simulated an ion current flow through a flexible nanopore using cations and an explicit extended simple point charge (SPC/E) water with molecular dynamics simulation. The simulation voltages range goes beyond the usual ionic channel measurements (± 1 V) and yields useful information about density profiles, current density distribution and current–voltage (I–V) characteristics.

Keywords: confinement; rectangular nanopore; external electric potential field; cation transport

1. Introduction

The transport of ions in a solution confined in nano-metre scale is critical for the function of inorganic and biological membranes. Therefore, it is important to study the effect of nano-confinement of ionic transport by computer simulation. To reduce computational time due to the fact that porous electrodes and biological ionic channels have complex geometry, simple electrolyte models can be used [1]. The studies of electrolyte solutions at a microscopic level have almost exclusively been performed at highly diluted concentrations in the last two decades [2]. Studying the influence of finite truncations of Coulomb forces on the structure of the aqueous dilutions of Cl^+ and Br^- at infinite dilution [3], some caution in making such direct comparison of these results with the experimental measurements should be applied. The experiments are by necessity carried out at much higher salt concentrations. In related problems, at higher densities, molecular dynamics (MD) simulation gives reliable results for transport properties of model electrolytes confined in nanopore [4]. With regard to the study of the electric migration of ions in the framework of the solvent primitive model, it is desirable to study the mobility of ions in a constant flux under a chemical potential gradient. This technique requires the set up of two reservoirs whose concentrations are maintained by grand canonical insertions/deletions [5]. Non-equilibrium molecular dynamics (NEMD) that determine the transport coefficients from the response of the system to an applied field have been discussed [6]. One approach is to move ions at constant flux in nanopore by potential gradient [7]. The other is to move ions under an axial electric gradient, which gives rise to net electric current and dissipation of energy. The application of the NEMD technique to the migration of low density primitive model electrolytes has been done. Driven by a constant uniform electric field applied in the axial direction of the nanopore, these MD simulations study the migrations of large cation concentrations, as reported [1,8–12]. More recently, a new NEMD method based on the transient-time correlation function formalism has been used to determine the current and conductivity of confined fluids subjected to an electric field [13,14].

However, at the present time, all the investigation was done in the electric range (− 1, 1 V) of the biological ionic channel. Therefore, the aim of this work is to analyse the response I–V curve of the system produced by an external electric field in a range that goes beyond the usual measurements applied to large Na^+ and K^+ concentrations in aqueous solution.

2. Models and simulations methods

The simulation set-up was similar to that described in earlier articles [4,15–16]. Initially we had 800 SPC/E [17] water molecules with initial density of 0.928 g/cm^3 as solvent, inside of the prismatic nanopore. In order to maintain the electro-neutrality of the system, the GROMOS87 package [18] has a code that replaces solvent molecules by atomic ions by placing the ion at the position of oxygen atom of a solvent molecule. Substitution of solvent molecules by positive and negative ions respectively is carried out for solvent positions with lowest and highest Coulomb potential respectively, or randomly. Consequently, we converted 100 water SPC/E molecules of the solvent into 50 ions and 50 counter-ions as solute, so that the counter-ions match the ions charge exactly. The prismatic surface is a network (3.4 × 3.0 × 3.0 nm, net constant 0.131 nm) of 2484 van der Waals particles. The van der Waals particles used were oxygen atoms, which were fixed by harmonic force (force

---

*Corresponding author. Email: maranon@fisica.unlp.edu.ar

ISSN 0892-7022 print/ISSN 1029-0435 online

DOI: 10.1080/08927020802488073
http://www.informaworld.com

constant = 80) to each network node. The counter-ions of Na·and K· used were the van der Waals particles with the same parameter and atomic mass but with negative charge corresponding to the Na and K cations. Potentials fields and configuration energies were computed using a modified GROMOS87 package for all types of particles (cations, counter-ions, atoms and van der Waals particles).

By NVT ensemble simulation, the transport properties of ions and counter-ions were calculated, applying a constant uniform electric field E_x along the axial direction of the nanopore. Under the external field, the charged particles move and after some simulation time steps generate an average constant current. Since the external electric field does work on the system as a consequence of the multiple collision with water molecules, counter-ions and van der Waals particles, the heat generated by the external electric field was removed by adding a constraint parameter (Gaussian thermostat) in non-Newtonian equations of motion [9,19,20]. The induced electric current density J_x in the axial direction in response to the applied electric field is

$$J_x = \frac{1}{\mathrm{Vol}} \sum_{i=1}^{N} q_i V_{i,x}, \tag{1}$$

where q_i is the charge and $V_{i,x}$ is the axial component of the ith ion, Vol is the volume of the pore and N is the total number of ions. In spite of that, the ionic concentration of the simulation cell is maintained by the axial periodic boundary condition, although fluctuations in current and motion of ions are detected over a long enough period of time. Consequently, the ion current is averaged after some simulation time steps. The temperature T of the non-equilibrium iso-kinetic system is obtained through the constraint [9] equation

$$T = \frac{1}{3Nmk_\mathrm{B}} \sum_{i=1}^{N} (\mathbf{p}_i - ((mq_iJ_x)/q_i\rho)\mathbf{e}_x)^2, \tag{2}$$

where $\mathbf{p}_i$ is the momentum vectors of the ith ion, $\mathbf{e}_i$ is the unit vector in the axial direction, m_i is the ion mass, N is the total number of ions in the system, $\rho = N/\mathrm{Vol}$ is the number density and k_B is the Boltzmann constant.

There are other ways of defining the thermostatic temperature of ions in terms of the position only (Equation (2)) in this non-equilibrium system, as shown [21]. This choice has a different effect on the value of the ions' density current (Equation (1)). This configurational expression for temperature [21] has advantages over any other formulation.

3. Results and discussion

3.1 Densities profiles

To study density profiles behaviour for Na and K ions in an aqueous solution, a series of different simulations were performed over a range of external applied voltages varying from −15 to 15 V in the nanopore. Since density profiles display quite similar pictures in all volts ranges for each ion, Figure 1 shows the pictures for 1 and 15 V only. The case of the Na ion, the density function distribution is closed to the nanopore axis while those of water molecules remain too near to the hydrophobic wall as in references [4,15]. In contrast, it can be observed that K ions and water molecules show different density profiles than those presented in [4,15], because the density profiles for K ions and water molecules fill nearly all the cross-sectional area of the nanopore. A plausible explanation of this different behaviour could be provided by the hydration number $n(r)_\infty$ [22] and the cation–water interaction for the K ion that are given in Table 1. Column 2 gives the hydration number of the K ion which weakly increases for large voltages. With regards to cation–water interaction, column 3 from 0.01 V gives values much lower than 0 V. In other words, with the increase of K ion kinetic energy by applying electric potential, the K ion solvation spheres interchange more water molecules with the aqueous solution, so that the water molecules spread through all the nanapore volume. By contrast, Na cation–water interactions are almost constant over all the voltage range, with an average value of -1.5×10 kJ/mol, the Na ion remaining near the nanopore axe as 0 V [15].

3.2 Current density distributions

The simple electrolyte model is formed with particles, and so the displacement of the ions in it is to a large extent hindered by counter-ions and solvent water. Consequently, the small electric field strength applied produces weak current density with large statistical errors. For all this, we investigated the inhomogeneity of the current density of the ions under electric field for 0–15 V and reverse sense in the pore. As a result of this study, a close up of Figure 2 shows only the current density of 1, 5, 10 and 15 V for both cations, Na and K, and correspondents reverse sense in spite of they are quite similar. We noted that the four pictures of current density distribution for the K ion have similar growing profiles, it shows two peaks near the wall and a valley at the axe of the nanopore. Moreover, current density is more enhanced near the wall than the axe of the nanopore. These results must be robust in potassium ion. Meanwhile, for the Na ion it also shows two peaks but it is given an irregular profile due to the influence of the flexible nanopore walls except for 1 V. Considering the different behaviour of both cations, current density could be roughly correlated with correspondent density profile for all voltages in Figure 1; for density profile peaks for K ion correspond to two similar symmetric current density peaks. Conversely, for all voltages, an irregular density profile for Na ion corresponds to an asymmetric current density except for 1 V. Finally, we noted that the

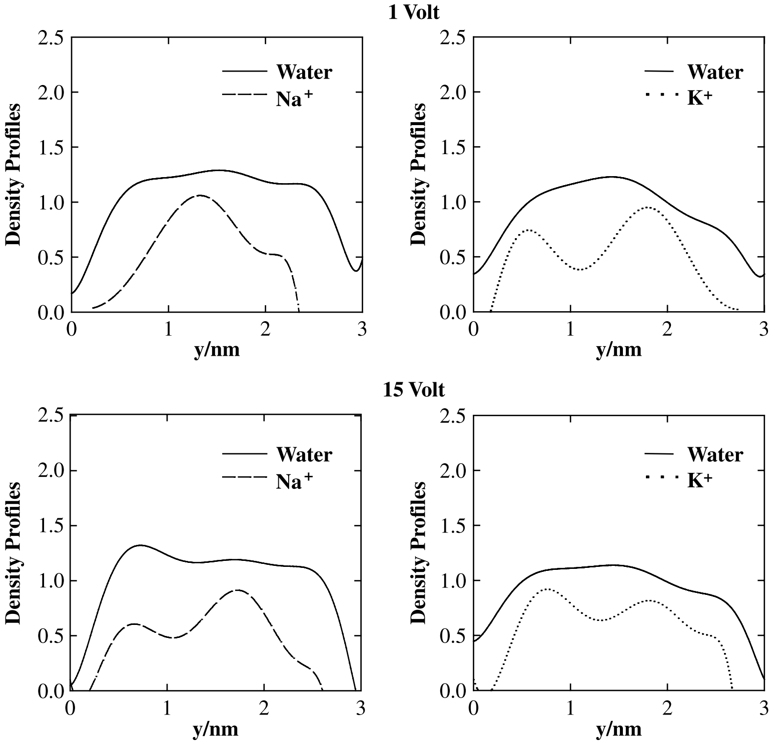

Figure 1. Radial distribution functions of ion–oxygen and bulk water of five different ion ratios in aqueous solution: (solid line) water, (dashed line) Na^+ and (dotted line) K^+.

confinement correlates the density profile (Figure 1) and current density distribution (Figure 2) for all voltages.

One question that remains to be discussed in Figure 2 is the different quantities of current density of Na and K ions in an aqueous solution under an electric field for all voltages and the comparison between them. Then, the average value calculation of the current density is made for both cations, as well as the relation between them. So, the result is shown in Table 2, where the second column is the current density average value of the Na ion and the third column, the corresponding values for the K ion. Lastly, the fourth column gives us the quotient of the average values between Na and K ions. We noted that for 1 V, the quotient of averages value for Na ion is 4.67 times that the average value for the K ion. Then, the quotient goes down to a weak 1.41 times at 15 V. The weak current density of the Na ion at 1 V is free of wall–ion interaction, giving two symmetric peaks weakly dominated by counter-ion coulombic interaction and water molecule collisions. Instead of the K ion, since its mass and volume are larger than those of the Na ion, the counter-ions and water molecules drastically reduce the current density to stabilise its symmetry. Following, for larger electric field strength, the average value of the current density for the Na ion becomes asymmetric and lightly higher than that for the K ion.

Table 1. Average hydration number of water molecules for K^+ first shell and cation (K^+)–water interaction versus applied electric potential.

Electric potential (V)	Hydration number	K^+–water interaction (kJ/mol)
0.00	7.1	-1.50×10^5
0.01	7.2	-1.42×10^4
1.00	7.3	-1.38×10^4
15.00	7.4	-1.12×10^4

3.3 *Ionic current curves*

Because ion currents are so small at low applied potentials, it takes large amounts of simulation time out of our computation limits to gain reliable statistics. For this reason values lower than 0.5 V and − 0.5 mV are not of interest to us, because this zone has already been studied by many authors [23–30]. Thus, due to large applied potential, ion motions along the axial direction within the channel are quite uniform (Figure 2).

The average ionic current of ions through the nanopores is shown as a function of applied potential. Figure 3 (inset of Figure 3) displays the current–voltage (I–V) curves of Na and K ions. In both (I–V) curves, it can be observed that, from values > -1 and < 1 V, they are quasi-linear, corresponding to organic channels that

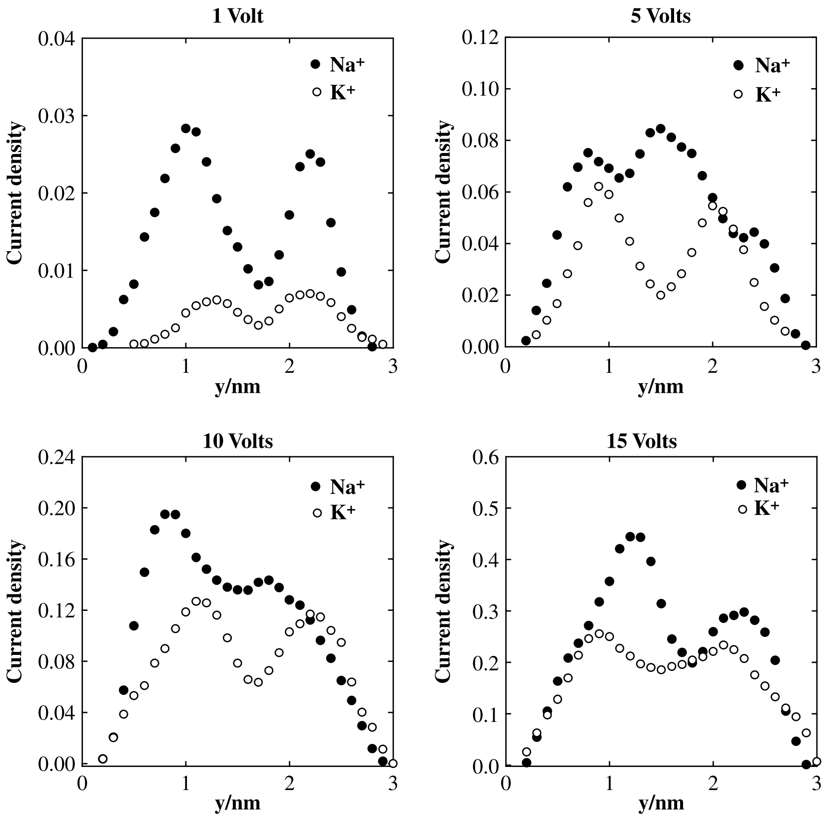

Figure 2. Na^+ and K^+ cations current density for 1, 5, 10 and 15 V: (dark circle) Na^+ and (circumference) K^+.

were studied exhaustively experimentally, using continuous theory and MD [10,20–27, and references therein]. Figure 3 shows, in spite of the lower statistic values, that (*I*–*V*) curves are slightly asymmetric, with the K ion curve more asymmetric than the Na ion. These results could be due to many questions: confinement effect, ions dimension and solvation energy. The solvation energy of the K ion is more perfect than that of the Na ion. Thus, the outward current is greater than the inward current for K ions. On the contrary, the smaller Na ions are not as perfectly solvated; consequently the Na cation $I–V$ curve is cut at right side of 0 V. These results are confirmed in part by papers [23,24,28]. The robustness of the quasi-linear zone suggests that the pore might serve as nano-rectifier current by geometrical consideration and charge distribution in the pore wall for different external potential drives.

Table 2. Average values of the Na^+ and K^+ current density distribution and their corresponding quotient as a function of electrical potential.

Electric potential (V)	Na^+ current density average value	K^+ current density average value	Average value Na^+/ average value K^+
1	0.014	0.003	4.67
5	0.051	0.033	1.55
10	0.110	0.071	1.55
15	0.237	0.168	1.41

Following our analysis of the (*I*–*V*) curves (Figure 3), it is similar in that Ca and Na ions obtained by Brownian dynamics MD simulation [23,24] and with less coincident current–voltage relationships were obtained experimentally for the same ions [31]. These findings and our $I–V$ relation in a range beyond the usual measurements suggest that it could be associated with the sinh function [32]

$$I = a \cdot \sinh(b \cdot V) \qquad (3)$$

writing a mathematical relation between I and V as follows, where I is the current, V is the electric potential and a and b are two parameters. Recently, by using a kinetic model [33], a similar $I–V$ functional form to (3) for a series of monovalent ions was obtained [34]. The curves attempt to fit by function (3) adjusting a and b parameters. In our case, the adjusted parameters yield for Na ion $a = 2.965$, $b = 0.144$ and K ion $a = 2.663$ and $b = 0.199$. Figure 4 shows: (a) Na ion (*I*–*V*) and the hyperbolic adjusted curve; (b) K ion (*I*–*V*) and the corresponding hyperbolic adjusted curve. Moreover, we

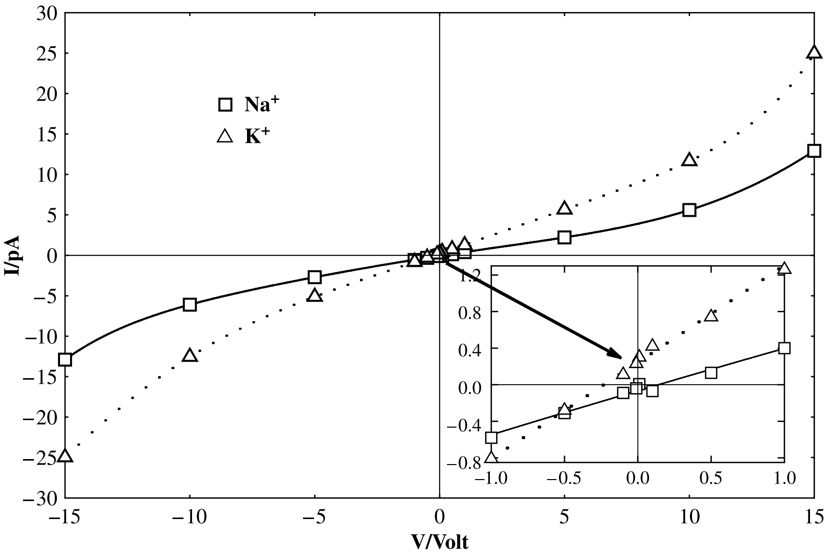

Figure 3. Na^+ and K^+ cations $I–V$ current voltage curves for positive and reversal electric potential. In the range of electric potential $(-15 \le \text{volts} \le 15)$ and the inset in four quadrant between $(-1 \le \text{volts} \le 1)$ range: (solid line) Na^+ regression curve, (dotted line) K^+ regression curve, (square) Na^+ and (triangle-up) K^+.

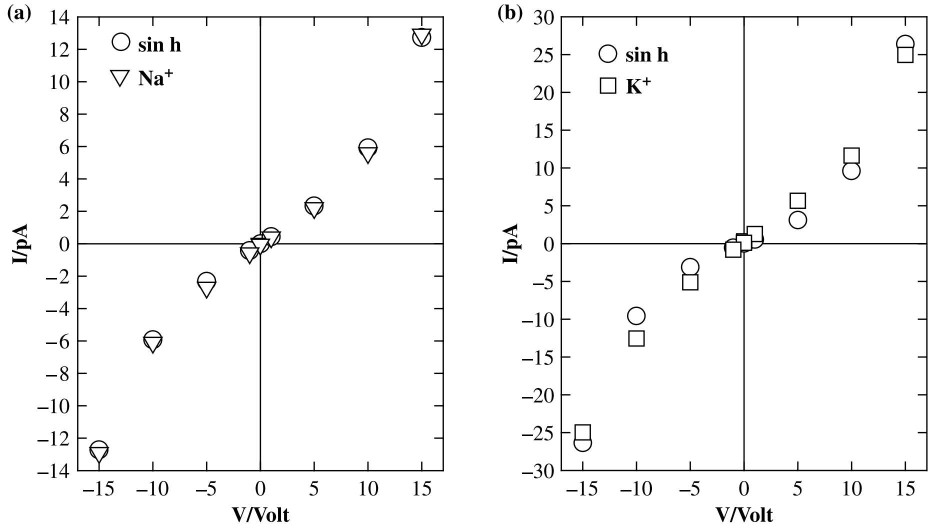

Figure 4. Na^+ and K^+ cations $I–V$ current voltage curves and the $I–V$ current voltage curves obtained with Equation (2) with a and b adjusted parameters: picture (a) (circumference) Equation (2) ($a = 2.965$, $b = 0.144$) and (triangle-down) Na^+ and picture (b) (circumference) Equation (2) ($a = 2.663$, $b = 0.199$) and (square) K^+.

note that, for the same ion concentration, the adjusting of the Na ion is good enough. Meanwhile, since the K ion has greater volume than the Na ion, the adjustment is not sufficiently good. We think that the adjustment of a and b parameters depends on other factors, such as ion concentration, two or more ions in solution, dimension and form of the nanopores, symmetric nanopores with asymmetric charge distribution. As we noted before, by using the configurational thermostat [36] for high voltages, greater deviation from the linear response could be obtained, and the adjustment of the corresponding a and b parameter gives us the $\sinh$ law.

4. Conclusions

A system with mobile ions and water molecules within a channel and wall atoms would obviously require much more computer processor time in MD simulation. However, one advantage of explicit solvation is that there is no need to employ artificial methods to represent a local dielectric constant. By using an external electric field of pore, we have given quantitative explanations to the ($I-V$) curves in a flexible nanopore for two monovalent ions. We have also computed the ion current flow through a simple nanopore model. Figure 2 shows one remarkable current flux profile, because for all voltages it can be associated with the skin effect of the ohmic conductor. By using the average value of the current density profile for both cations for all voltages, it was observed that for the quotient of the average values between Na and K ions, for 1 V, the quotient of the average value of the Na ion is 4.67 times the average value of the K ion. Then, the quotient falls to a weak 1.41 times at 15 V. Figure 4 shows a novel law, sin h function of the ($I-V$) Equation (2), for confined ion current drive by an electric potential different from the solid conductor Ohm law.

For null electric field [15] shows a density profile, where the ions are distributed along the nanotube, near to the x-axis. Water molecules do not exhibit a shift from the axis of the nanotube and they are repelled by hydrophobic elastic walls. The profile centres of the water molecules are not avoided by the ions. Therefore, we suppose that this trend is due to the fact that there is a competition between ion hydration and ion interaction which depends of the size of the ions. Then, by application of high external electrical field a self-organisation on cations, Na and K, and the correspondent counter-ions were induced. Figure 1 shows that the ionic density profile is not totally unfolded only in two density profiles, and Figure 2 shows a two-current lane, where solvated ions flow parallel but without perpendicular component to field applied. In the case of the K ion, according to Table 1, the first solvation sphere has on average seven water molecules with residence time for each molecule of [15] 6.2 and 11.7 ps for Na ion. These values are the averaged time that a water molecule remains in the solvation sphere to the end that exchanges between ion and solvent. Besides, the density profiles of the solvent for null field [15] and for different values of applied fields, Figure 1 has a similar aspect. The same results are obtained for counter-ions with lanes generated by electric field intercalated between ion lanes [35,36] with current in contrary sense. Finally, [33] shows that using a configurational thermostat instead of a kinetic thermostat constitutes a much safer way to account for heat dissipation in non-equilibrium system.

Acknowledgements

This work was partly supported by the CONICET, Argentina. J.M.D.L. is a senior researcher of CONICET, Argentina. The authors are grateful to the referee for providing a bibliography about lane self-organisation.

References

[1] K.Y. Chan, Y.W. AI Tang, and I. Szalai, *Ion transport in simple nanopores*, Mol. Sim. 30 (2004), pp. 81–87.

[2] Y. Laudernet, *Using Car-Parrinelo molecular dynamics in order to improve classical simulations, Laboratoire Liquides Ioniques et Interfaces Chargees*, Universitie. Pierre et Marie Curie, France. Available at www.cineca.it/editions/ssc2003/minos/0029.pdf.

[3] C.L. Brooks III, *The influence of long-range force truncation on the thermodynamics of aqueous solutions*, J. Chem. Phys. 86 (1987), pp. 5156–5162.

[4] J. Marañón Di Leo and J. Marañón, *Confined ions and water in nanotube*, J. Mol. Struct. (Theochem) 709 (2004), pp. 163–167.

[5] G.S. Heffelfinger and F. Van Swol, *Diffusion in Lennard-Jones fluids using dual control volume grand canonical molecular dynamics simulation (DCV-GCMD)*, J. Chem. Phys. 11100 (1994), pp. 7548–7552.

[6] S.S. Sarman, D.J. Evans, and G.P. Morris, *Recent developments in non-Newtonian molecular dynamics*, Phys. Rep. 308 (1998), pp. 1–92.

[7] J. Dzubiella, R.J. Allen, and J.P. Hansen, *Electric field-controlled water permeation coupled to ion transport through a nanopore*, J. Chem. Phys. 120 (2004), pp. 5001–5004.

[8] P.S. Crozier, R.L. Rowley, N.B. Holladay, D. Henderson, and D.D. Busath, *Molecular dynamics simulation of continuous current flow through a model biological membrane channel*, Phys. Rev. Lett. 86 (2001), pp. 2467–2470.

[9] Y.W. Tang, I. Szalai, and K.W. Chan, *Diffusivity and conductivity of a primitive model electrolyte in a nanopore*, Mol. Phys. 99 (2001), pp. 309–314.

[10] Y.W. Tang, I. Szalai, and K.W. Chan, *Diffusivity and conductivity of a solvent primitive model electrolyte in a nanopore by equilibrium and nonequilibrium molecular dynamics simulations*, J. Chem. Phys. 105 (2001), pp. 9616–9623.

[11] Y.W. Tang, I. Szalai, and K.W. Chan, *Non-equilibrium molecular dynamics simulation study of the frequency dependent conductivity of a primitive model electrolyte in a nanopore*, Mol. Phys. 100 (2002), pp. 1497–1505.

[12] Y.W. Tang, K.W. Chan, and I. Szalai, *Structural and transport properties of an SPC/E electrolyte in a nanopore*, J. Phys. Chem. B 108 (2004), pp. 18204–18213.

[13] C. Desgranges and J. Delhommelle, *Molecular simulation of transport in nanopores: application of the transient-time correlation function formalism*, Phys. Rev. E 77 (2008), 027701.

[14] C. Desgranges and J. Delhommelle, *Estimating the conductivity of a nanoconfined liquid subjected to an experimentally accessible external field*, Mol. Sim. 34 (2008), pp. 277–281.

[15] J. Marañón Di Leo and J. Marañón, *Confined Na$^+$ and K$^+$ ions in an aqueous solution*, Chem. Phys. Lett. 404 (2005), pp. 257–262, and references therein.

[16] J. Marañón Di Leo and J. Marañón, *Hydration and diffusion of cations in nanopores*, J. Mol. Struct. (Theochem) 729 (2005), pp. 53–57.

[17] H.J.C. Berendsen, J.R. Grigera, and T. Straatsma, *The Missing term in effective pair potentials*, J. Phys. Chem. 91 (1987), pp. 6269–6271.

[18] W.F. van Gusteren and H.J.C. Berendsen, *GROningen MOlecular Simulation package*. Available from Biomos n.v. Ninborgh 16, 4767 AG Groningen.

[19] D.J. Evans and G.P. Morris, *Statistical Mechanics of Nonequilibrium Liquids*, Academic Press, London, 1990.

[20] I.M. Svishchev and P.G. Kusalik, *Dynamical properties of Coulombic systems at low densities: computer simulation results*, Phys. A 192 (1993), pp. 628–646.

[21] J. Petravic and J. Delhommelle, *Conductivity of molten sodium chloride and its supercritical vapor in strong dc electric fields*, J. Chem. Phys. 115 (2003), pp. 7477–7845.

[22] D. Duh, D.N. Perera, and A.D.J. Haymet, *Structure and properties of the CF1 central force model of water: integral equation theory*, J. Chem. Phys. 102 (1995), pp. 3736–3746.

[23] T.W. Allen, M. Hoyles, S. Kuyucak, and S.H. Chung, *Molecular and Brownian dynamics study of ion selectivity*, Chem. Phys. Lett. 313 (1999), pp. 358–365.

[24] B. Corry, T.W. Allen, S. Kuyucack, and S.H. Chung, *Mechanism of permeation and selectivity in calcium channels*, Biophys. J. 80 (2001), pp. 195–214.

[25] P. Ramirez, S. Mafe, V.M. Aguilella, and A. Alcaraz, *Synthetic nanopores with fixed charges: an electro-diffusion model for ionic transport*, Phys. Rev. E 68 (2003), 011910.

[26] S. Mafe, J. Pellicer, and J. Cervera, *Kinetic modelling of ion conduction in KcsA potassium channels*, J. Chem. Phys. 122 (2005), 204712.

[27] I. Cozmuta, J.T. O'Keeffe, D. Bose, and V. Stolc, *Hybrid MD-Nerst Plank model of α-hemolysin conductance properties*, Mol. Sim. 31 (2005), pp. 79–93.

[28] Z. Siwy, I.D. Kosinska, A. Fulinski, and C.R. Martin, *Asymmetric diffusion through synthetic nanopores*, Phys. Rev. Lett. 94 (2005), 048102.

[29] J. Cervera, B. Schiedt, R. Neumann, S. Mafe, and P. Ramirez, *Ion conduction, rectification, and selectivity in single conical nanopores*, J. Chem. Phys. 124 (2006), 104706.

[30] I.D. Kosinska, *How the asymmetry of internal potential influences the shape of I-V characteristic of nanochannels*, J. Chem. Phys. 124 (2006), 244707.

[31] R.L. Rosenberg and X.H. Chen, *Characterization and localization of two ion-binding sites within the pore of cardiac L-type calcium channels*, J. Genet. Physiol. 97 (1991), pp. 1207–1225.

[32] M.R. Spiegel, *Mathematical Handbook of Formulas and Tables*, MacGraw-Hill Inc, New York, 1968.

[33] P.H. Nelson, *Modelling the concentration-dependent permeation modes of the KcsA potassium ion channel*, Phys. Rev. E 68 (2003), 061908.

[34] S. Mafe and J. Pellicer, *Ion conduction in KcsA potassium channel analyzed with a minimal kinetic model*, J. Chem. Phys. 122 (2005), 204712.

[35] J. Dzubiella, G.P. Hoffmann, and H. Lowen, *Lane formation in colloidal mixtures driven by an external field*, Phys. Rev. E 65 (2002), 021402.

[36] J. Delhommelle, *Should 'lane formation' occur systematically in driven liquids and colloids?*, Phys. Rev. E 71 (2005), 016705.